CrossMark

Tectonic stress regime in the 2003–2004 and 2012–2015 earthquake swarms in the Ubaye Valley, French Alps

Lucia Fojtíková[1,2] and Václav Vavryčuk[3]

Abstract—We study two earthquake swarms that occurred in the Ubaye Valley, French Alps within the past decade: the 2003–2004 earthquake swarm with the strongest shock of magnitude ML = 2.7, and the 2012–2015 earthquake swarm with the strongest shock of magnitude ML = 4.8. The 2003–2004 seismic activity clustered along a 9-km-long rupture zone at depth between 3 and 8 km. The 2012–2015 activity occurred a few kilometres to the northwest from the previous one. We applied the iterative joint inversion for stress and fault orientations developed by Vavryčuk (2014) to focal mechanisms of 74 events of the 2003–2004 swarm and of 13 strongest events of the 2012–2015 swarm. The retrieved stress regime is consistent for both seismic activities. The σ_3 principal axis is nearly horizontal with azimuth of $\sim 103°$. The σ_1 and σ_2 principal axes are inclined and their stress magnitudes are similar. The active faults are optimally oriented for shear faulting with respect to tectonic stress and differ from major fault systems known from geological mapping in the region. The estimated low value of friction coefficient at the faults 0.2–0.3 supports an idea of seismic activity triggered or strongly affected by presence of fluids.

Key words: Ubaye Valley, south-western Alps, earthquake swarm, focal mechanism, stress inversion, fluids.

1. Introduction

Earthquake swarms have been observed in volcanic regions (Hensch et al. 2008; Vidale et al. 2006), in geothermal areas with quaternary volcanism (Fischer and Horálek, 2003; Fischer et al. 2014) and in non-volcanic areas with fluid-driven seismicity (Got et al. 2011) where fluid overpressure or fluid migration can be a trigger mechanism of seismic activity. Earthquake swarms are characterized as sequences

with no clear mainshock (Hill 1977; Scholz 2002); however, they can display a great variety and complex behaviour depending on tectonic environment (Shelly et al. 2013; Vavryčuk et al. 2013; Thouvenot et al. 2016; Yoshida et al. 2016; Vavryčuk and Hrubcová 2017).

The Ubaye Valley is one of the most seismically active areas in the French Alps. Two earthquake swarms occurred in this area within the past decade. The first earthquake swarm occurred in 2003–2004 with magnitude of the strongest event of ML = 2.7. The activity clustered along a 9-km-long rupture zone across the Ubaye Valley at a depth range between 3 and 8 km (Jenatton et al. 2007). The second earthquake swarm occurred in the period of 2012–2015 being located a few kilometres to the northwest from the previous one. It was initiated by a shock with ML = 4.3 and reactivated after 2 years by another ML = 4.8 shock with an identical epicentre but of a deeper focus (Thouvenot et al. 2016). Earthquakes in the area are monitored since 1994 by the SISMALP seismic network, which consists of 44 short-period one- or three-component seismic stations. The majority of the stations operate in a triggered mode.

In this paper, we study stress regime in the Ubaye Valley using a seismic activity occurring during the two last earthquake swarms. We apply a new recently developed stress inversion technique, the iterative joint inversion for stress and fault orientations (Vavryčuk 2014), in order to find a possible stress variation, to identify the orientation of activated faults and to evaluate fault friction and instability of the active faults. We compare our results with those published previously to assess uncertainties in the retrieved stress. Finally, we discuss a possible role of fluids in triggering the studied swarm activity.

[1] Institute of Rock Structure and Mechanics, The Czech Academy of Sciences, V Holešovičkách 94/41, 182 09 Prague, Czech Republic. E-mail: fojtikova@irsm.cas.cz

[2] Earth Science Institute, Slovak Academy of Sciences, Dúbravská cesta 9, 84528 Bratislava, Slovakia.

[3] Institute of Geophysics, The Czech Academy of Sciences, Boční II/1401, 141 00 Prague, Czech Republic.

2. Seismotectonic Settings

The western Alpine arc originated during the Cretaceous orogenesis as a consequence of the continental collision between the European and Adriatic plates. The ongoing tectonics of the western and central Alps is characterized by a widespread extensional regime located in the core of the belt and a dominant transcurrent tectonic regime at the outer borders of the chain, with some local compressive areas (Sue et al. 2007). In addition, the western Alps are characterized by continuous orogen-perpendicular extension in the inner areas of the belt, and localized zones of compression/transpression at the outer boundaries of the belt, associated with strike-slip areas in external zones, and defining a large-scale fan pattern with orogen-perpendicular σ_1 axes (Delacou et al. 2004).

The study area is situated in the south-western Alps, in the Ubaye Valley and it is characterized by upper crustal seismicity at depths down to 12–15 km (Fig. 1). A recent moderate event, the Saint-Paul-sur-Ubaye earthquake, occurred in 1959 (Nicholas et al. 1998; Eva and Solarino 1998) succeeded by several earthquake swarms in 1978 (Frechet and Pavoni 1979), 1989 (Guyoton et al. 1990), 2003–2004, and in 2012–2015. The focal mechanisms of the strongest earthquakes in 1959 (ML = 5.3); 2003 (ML = 2.7); 2012 (ML = 4.3) and 2014 (ML = 4.8) are very similar: predominantly normal faulting with a small strike-slip component (see Fig. 1b). The Quaternary to present-day activity of the NW–SE faults is ascertained for one of these faults, the so-called Jausiers-Tinée fault (Sanchez et al. 2010a, b). The presence of several hot springs located few tens of kilometres from the study area suggests that the activity might have a relation to fluid circulation within the bedrock (Daniel et al. 2011).

Orientations of the principal axes of the regional tectonic stress inferred from a previous seismicity (e.g., Eva and Solarino, 1998; Delacou et al. 2004; Daniel et al. 2011; Leclère et al. 2012), GPS-related strain and seismic strain observations (e.g., Sue et al. 2007; Tesauro et al. 2006; Larroque et al. 2009), and geological mapping of main active fault systems indicate a complex tectonic history with a significant spatial variation of stress pattern (Sanchez et al.

2010b). Eva and Solarino (1998) analysed focal mechanisms of 86 earthquakes that occurred in the western Alpine arc in the period of 1983–1996. They pointed to a remarkable variation of the principal stress axes σ_1 and σ_2 along the Alpine arc. The σ_1 axis is characterized by a notable horizontal inclination. In addition, the magnitudes of the σ_1 and σ_2 stresses are comparable and the σ_3 axis is nearly horizontally oriented. The stress directions are characterized by slight to significant deviations from the expected compressional stress regime due to collision between the Adriatic and European plates. These stress inversion results appear to be in agreement with the geodynamic uplift associated with the regional-scale thrusting process, which has reactivated, as normal faults, pre-existing shallow structures (Labaume et al. 1989). The distribution of stress orientations in the western Alpine arc was calculated by Delacou et al. (2004) and the orientation of the main stress axes shows a rotation along the Alpine arc.

3. The 2003–2004 Earthquake Swarm in the Ubaye Valley

The swarm started in January 2003. It reached the maximum activity in October 2003 with three shocks (ML = 2.7) and lasted till December 2004. A weak activity with a few more low-magnitude shocks occurred also in 2005. The seismic activity consisted of more than 16,000 earthquake foci which formed a 9-km-long cluster with a NW–SE strike at depth ranging from 3 to 8 km with the most intense activity between 6 and 8 km (Jenatton et al. 2007; Leclère et al. 2012). The activity initiated in the central part of the rupture zone, diffused to its periphery, and eventually concentrated in its southeastern deeper part where the late 2005 shocks are also located. The corresponding hydraulic diffusivity is about 0.05 $m^2 \ s^{-1}$ (Jenatton et al. 2007). The Gutenberg-Richter b-value significantly varied from 1.0 at the beginning to 1.5 when the swarm reached its climax. The focal mechanisms for the largest shocks show either normal faulting with the southwest–northeast-trending extension direction or northwest-southeast strike slip with a right-lateral displacement (see Fig. 1b).
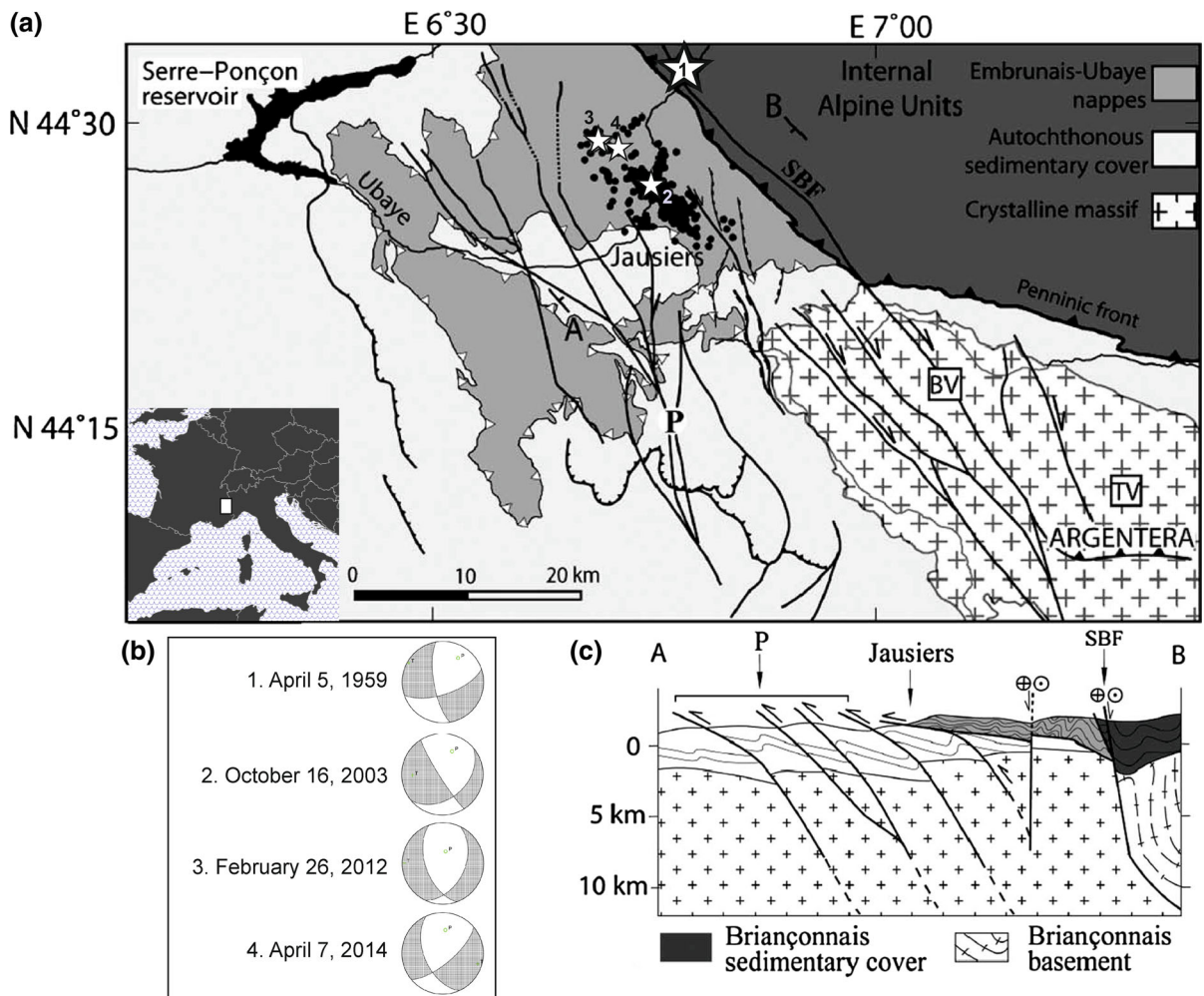
Figure 1

Geological setting of the study area after Leclère et al. (2013), modified. **a** Simplified geological map. *SBF* Serenne-Bersezio fault, *P* Parpaillon faults, *BV* Bagni di Vinadio thermal springs, *TV* Terme di Valdieri thermal springs. The star 1 indicates the location of the epicentre of the 1959 ML 5.3 Saint-Paul-sur-Ubaye earthquake (Nicolas et al. 1998). The stars 2, 3 and 4 indicate the locations of the epicentres of the 2003 ML 2.7, 2012 ML 4.3 and 2014 ML 4.8 earthquakes, respectively (Jenatton et al. 2007; Thouvenot et al. 2016). Black dots show epicentres of the 2003–2004 Ubaye swarm. **b** Focal mechanisms of the strongest events shown in (**a**). Mechanisms were adopted from: 1 Eva and Solarino (1998); 2, 3 Jenatton et al. (2007); 4. Thouvenot et al. (2016). **c** Cross section A–B showing the relationships between the crystalline basement, the autochthonous sedimentary cover and the Embrunais-Ubayenappes, after Leclère et al. (2013)

Leclère et al. (2012) inverted focal mechanisms of the largest events of the 2003–2004 earthquake swarm for a regional stress. They show that the axis of the maximum principal stress σ_1 is nearly horizontal deviating by 63° from the fault plane. The intermediate principal stress σ_2 axis is almost parallel to the fault plane. The 2-D analysis with a static coefficient of friction of 0.4 (consistent with the presence of phyllosilicate-rich gouges at depth)

indicates that the fault has a strike of 130° and a dip of 80°. This fault orientation is not optimum for the fault to be activated by the tectonic stress in the region; hence the fault reactivation would be possible only under extreme pore-fluid pressure excess in the hypocentral zone (6–7 km below the surface).

Leclère et al. (2013) provided an estimation of fluid pressure along the fault planes based on the Mohr–Coulomb failure criteria. They show that the

fluid overpressure required to reactivate the cohesionless fault planes varies with time and being close to 35 MPa at the inception of the swarm. The overpressure increases up to 55 MPa during the burst of the seismic activity and finally drops down to 20 MPa at the end of the seismic crisis. Leclère et al. (2013) also conclude that the moderate fluid overpressure at the swarm inception could enable the reactivation of normal, transtensional and strike-slip faults while the development of higher fluid overpressure during the burst of seismic activity progressively enables the reactivation of further misoriented normal, transtensional and transpressional faults.

4. The 2012–2015 Earthquake Swarm in the Ubaye Valley

The 2012–2015 earthquake swarm is peculiar because it was initiated by the ML = 4.3 shock and reactivated after two years by another ML = 4.8 shock with the identical epicentre but at greater depth. The active area lies several kilometres NW from the focal zone of the 2003-2004 earthquake swarm. In total 13.000 earthquakes were recorded and 3.000 earthquakes were relocated using the double-difference method (Thouvenot et al. 2016). The seismicity aligned along a 11-km-long zone with a NNW–SSE strike at depth between 4 and 11 km. Focal mechanisms of 13 earthquakes with ML ≥ 3 confirm the complexity of the swarm geometry, although the fault planes for the two "mainshocks" are very consistent (strikes of 156° and 160°, dips of 52° and 55°, respectively), with a clear normal faulting and a slight dextral strike-slip component. Thouvenot et al. (2016) calculated striking and dipping of the swarm focal zone. The resultant strike and dip are 165° and 80°, respectively. The hydraulic diffusivity of 0.05 m² s⁻¹ found for the 2003–2004 swarm fits reasonably well the 2012 data, but not the 2014 reactivation sequence. The activity observed over the 3.5-year period does not abide by the Omori law as could be expected for the ML 4.3 and 4.8 shocks. The activity is basically swarm-like but with complexities originated in the occurrence of two strong shocks, each having its own foreshocks and aftershocks superimposing onto the swarm.

5. The Method of the Iterative Joint Inversion for Stress and Fault Orientations

The fracture process on the fault depends on shear stress, pore-fluid pressure, fault friction and cohesion in the focal zone (Vavryčuk 2014). In addition, the orientation of the fault with respect to the principal stress directions governs susceptibility of the fault to be ruptured (Vavryčuk 2011). If we know focal mechanisms for a set of earthquakes that occurred in the focal zone, we can invert them for tectonic stress (e.g., Michael 1984, 1987; Angelier 1984; Gephart and Forsyth 1984; Zoback 1992). The stress inversion is based on several assumptions (Maury et al. 2013; Vavryčuk 2015): (1) the stress is uniform in the region, (2) the earthquakes occur on faults with varying orientations, (3) the slip vector points in the direction of the shear traction on the fault (the so-called Wallace-Bott hypothesis; see, Wallace 1951; Bott 1959) and (4) the earthquakes do not interact with each other and do not disturb the background tectonic stress. Under these conditions the stress inversion allows us to estimate the orientation of the principal stress axes and the shape (stress) ratio

$$R = \frac{\sigma_1 - \sigma_2}{\sigma_1 - \sigma_3} \qquad (1)$$

The assumptions of the stress inversion look apparently very restrictive but analysis of real observations proves that they are well-satisfied in most cases, in particular, for local seismicity formed by weak or moderate earthquakes: (1) the background stress varies very smoothly even at regional distances, (2) the vertical stress gradient due to gravity and pore pressure projects mostly to the isotropic lithostatic pressure, which does not affect either the orientation of principal stress axes or the calculated stress ratio, and (3) the stress drop of weak earthquakes is negligible with respect to the background stress, so the earthquakes do not disturb it and can be considered as independent. Obviously, if seismicity covers a large seismic zone (horizontally or vertically) or a long time period, the spatial or temporal variations of stress can be observed. In this case, the area should be studied by subdividing into cells of similar stress regime and by inverting for stress in individual cells (Hardebeck and Michael 2006;

Vavryčuk 2006; Townend et al. 2012). As regards the stress variation with depth, it is also possible to invert for a vertical stress gradient if the activity samples a large depth range (Maury et al. 2013). Besides, if seismic sequences include strong earthquakes with magnitude greater than 5, the effects of the Coulomb stress produced by earthquakes cannot be neglected and some selection criteria for independent earthquakes should be applied to the input dataset (Maury et al. 2013; Martinez-Garzón et al. 2016a).

A common difficulty of stress inversions of focal mechanisms is an ambiguous choice of a fault plane from two nodal planes. Since incorrectly selected fault planes in focal mechanisms may bias the retrieved stress ratio (Vavryčuk 2015), the inversion can be improved by incorporating an algorithm for identifying the fault plane based on evaluating the fault instability I introduced by Vavryčuk (2011, 2014):

$$ I = \frac{\tau + \mu(\sigma + 1)}{\mu + \sqrt{1 + \mu^2}}, \qquad (2) $$

where τ and σ are the normalized shear and normal tractions on a fault

$$ \sigma = -n_1^2 - (1 - 2R)n_2^2 + n_3^2 \qquad (3) $$

$$ \tau = \sqrt{n_1^2 + (1 - 2R)^2 n_2^2 + n_3^2 - \left(n_1^2 + (1 - 2R)n_2^2 - n_3^2\right)^2} \qquad (4) $$

R is the stress ratio, μ is the friction coefficient and $\mathbf{n}$ is the fault normal evaluated in the coordinate system of the principal stress axes. The fault plane is identified with that nodal plane which has higher fault instability I. The fault instability measures the susceptibility of the fault to be activated by shear faulting with respect to its orientation in the given stress field. The optimally oriented fault attains instability I of 1. It is called the 'principal fault' and it deviates from the σ_1 axis by angle $\theta = \arctan \mu^{-1}$ being close to 30° (Vavryčuk, 2011). Since the fault instability I measures just how favourably oriented the fault is for shearing, it does not reflect whether the Mohr–Coulomb failure criterion is actually satisfied on the fault or not. Consequently, the fault instability I does not depend on the pore pressure, which is usually essential for satisfying the Mohr–Coulomb

failure criterion and for triggering the seismicity (Vavryčuk et al. 2013; Martinez-Garzón et al. 2016b).

As proposed by Vavryčuk (2014) the joint inversion for stress and fault orientations utilizing the instability concept is run in several iterations. In the first iteration, the stress is estimated using faults randomly selected from the nodal planes. The obtained stress serves for identifying the correct fault planes according to Eq. (2) and the stress inversion is run again. This process is repeated until it converges to the final value. Usually, about 5–10 iterations are sufficient for obtaining the final stress. The iterative joint stress inversion can be run using the open-access STRESSINVERSE code written in MATLAB (Vavryčuk, 2014).

6. Application to Data

The tectonic stress in the focal zone was computed by the STRESSINVERSE code using focal mechanisms of 74 events of the 2003–2004 swarm and of 13 strongest events of the 2012–2015 swarm, respectively. The focal mechanisms of 38 events of the 2003–2004 swarm were calculated by Jenatton et al. (2007, their Figs. 5 and 6). The set was further extended to 74 events by Leclère et al. (2013, their Figs. 4 and 5). The focal mechanisms of 13 ML ≥ 3.0 events of the 2012–2015 were calculated by Thouvenot et al. (2010, their Fig. 9 and Table 3). All focal mechanisms were computed by the FPFIT software (Reasenberg and Oppenheimer 1985) using the P-wave first-motion polarities. The minimum number of the P-wave polarities was 13 and 31 for the 2003–2004 and 2012–2015 swarm events, respectively. The majority of events in both datasets are characterized by strike-slip or normal focal mechanisms.

The results of the stress inversion are shown in Fig. 2 and summarized in Table 1. The focal mechanisms display a significant variability but the P and T axes form clusters which are separated and do not overlap. The P axes are more scattered than the T axes indicating that the σ_3 axis is better constrained than the σ_1 axis. The positions of fault planes in the Mohr's circle diagram are characterized by high
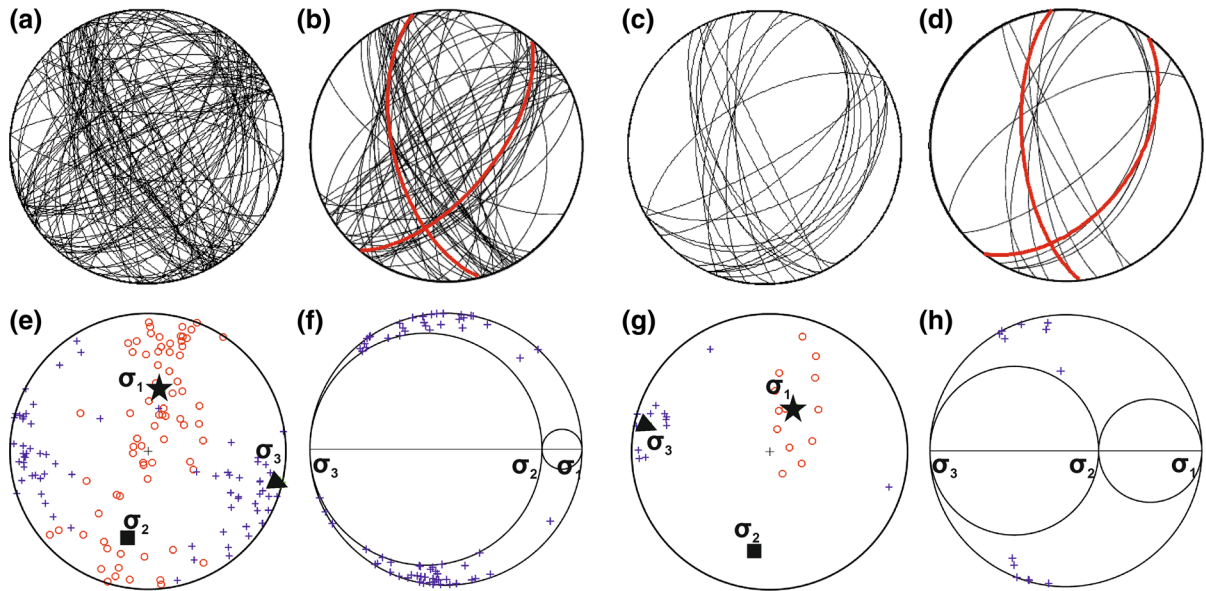
Figure 2
Iterative joint inversion for stress and fault orientations for the 2003–2004 swarm (four left panels) and the 2012–2015 swarm (four right panels). For the 2003–2004 seismic swarm: **a** nodal lines of the analysed events, **b** faults identified by the inversion. The red nodal lines denote the principal faults at the area (i.e., hypothetical faults optimally oriented for shear faulting in the given stress field). **e** P axes (red circles) and T axes (blue plus signs) and retrieved principal stress directions. **f** Mohr's circle diagram with positions of faults (plus signs). Panels **c, d, g, h** the same as panels **a, b, e, f** but for the 2012–2015 swarm, respectively

shear stress (Fig. 2f, h). Since the fault planes lie in the upper as well as lower half-planes, conjugate faults symmetrically oriented with respect to the maximum compression were activated. The both fault systems are highly unstable having orientation close to the principal faults (Vavryčuk 2011) calculated for this region. In addition, the optimum friction was determined during the inversion. High shear stress on faults (Fig. 2f, h) implies that the value of friction is rather low ($\sim$ 0.2–0.3) for both swarms.

The estimation of errors is provided by a repeated stress inversion of focal mechanisms contaminated by artificial noise. We use 100 realizations of random noise in the inversion. The level of noise of 10° corresponds to the estimated accuracy of input focal mechanisms. The inversion process is stopped after 6 iterations. For both seismic sequences, the stress is characterized by a mostly horizontal σ_3 axis; the σ_1 and σ_2 axes deviate from both horizontal and vertical directions (Fig. 3a). The value of the stress ratio is low: 0.15 ± 0.10 for the 2003–2004 swarm, and 0.38 ± 0.20 for the 2012–2015 swarm (see Table 1). The confidence limits are quite wide-spread because

the shape ratio is sensitive to the number of focal mechanisms inverted and to their accuracy (Fig. 3b, d). The low value of the shape ratio physically means that the σ_1 and σ_2 stresses are of similar magnitudes and thus the σ_1 and σ_2 axes cannot be easily distinguished. This causes large errors in their directions (see Table 1).

7. Discussion

Previous studies show that the south-western Alps display a complex pattern of tectonic stress (Fig. 4). Structural and geochronological investigations have provided evidence for the active character of the south-western Alps strike-slip system (Sanchez et al. 2010b).

For the 2003–2004 swarm, we retrieved the orientation of the principal stress axes σ_1, σ_2 and σ_3 (azimuth/plunge): 11°/53°, 195°/37° and 103°/2°, respectively (see Table 1). The error in the σ_3 axis is about 3° in azimuth as well as in plunge. The azimuth of the $\sigma_1 - \sigma_2$ plane is well constrained with the error

Table 1

Comparison of results of retrieved tectonic stress

Author/dataset	σ_1 Azimuth/Plunge	σ_2 Azimuth/Plunge	σ_3 Azimuth/Plunge	R
This paper, 2003–2004 swarm	11°/53° ± 30°	195°/37° ± 30°	103°/2° ± 3°	0.15 ± 0.10
This paper, 2012-2015 swarm,	29°/61° ± 45°	188°/27° ± 45°	283°/9° ± 10°	0.38 ± 0.20
Eva and Solarino (1998), B/West	54°/66°	160°/7°	253°/23°	0.5
Delacou et al. (2004), b3N	194°/71°	11°/19°	101°/1°	0.14
Delacou et al. (2004), b3S	335°/59°	139°/30°	233°/7°	0.52
Leclère et al. (2012), 2003–2004 swarm	13°/12°	153°/74°	281°/9°	0.30

Marks of areas in Delacou et al. (2004) are consistent with Fig. 4a. Note that the results of Eva and Solarino (1998) and Delacou et al. (2004) do not characterize the Ubaye Valley region only but they cover also its surroundings
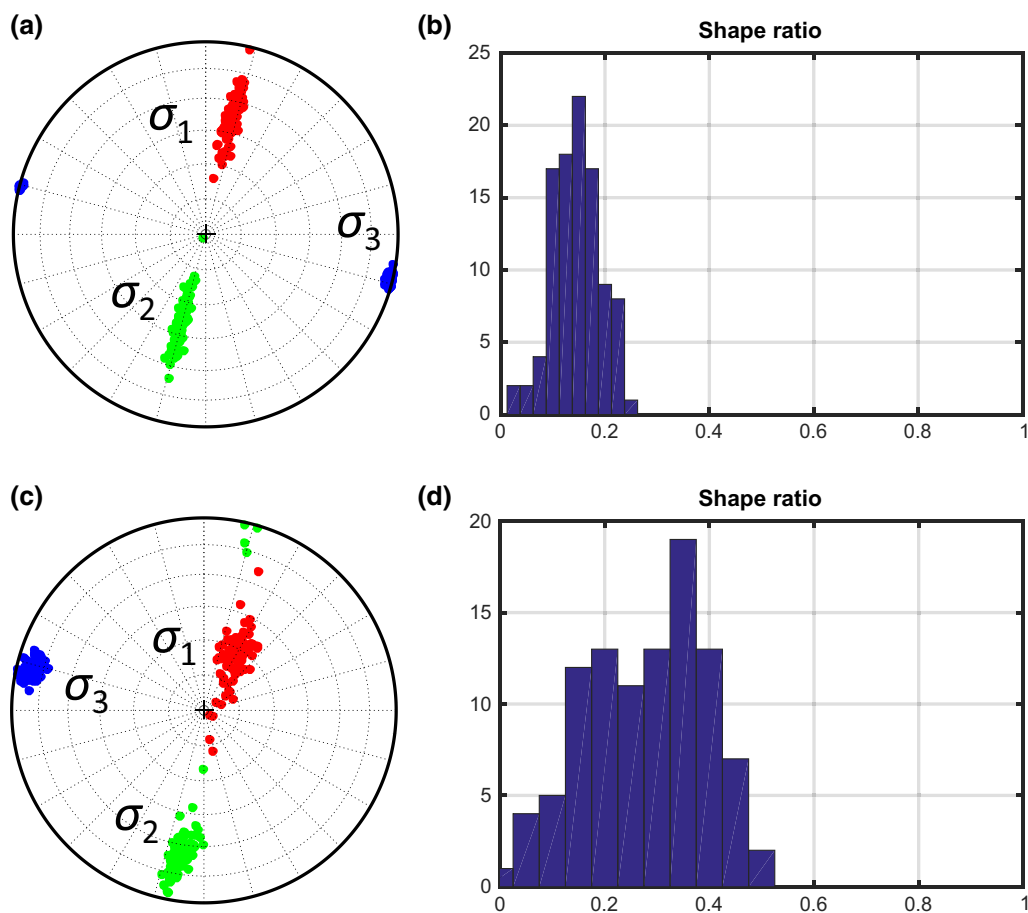

Figure 3

Confidence limits of the principal stress directions (*left*), and the shape ratio histograms (*right*) for the 2003–2004 swarm (**a**, **b**) and the 2012–2015 swarm (**c**, **d**), respectively

of 3°. The plunge within the plane is, however, quite uncertain with the error of about 30° at the 95% confidence level (see Fig. 3a). These results are

slightly different when compared to Leclère et al. (2012): the azimuth of σ_1 is similar but the plunge is different. Our analysis indicates that σ_1 and σ_2 can
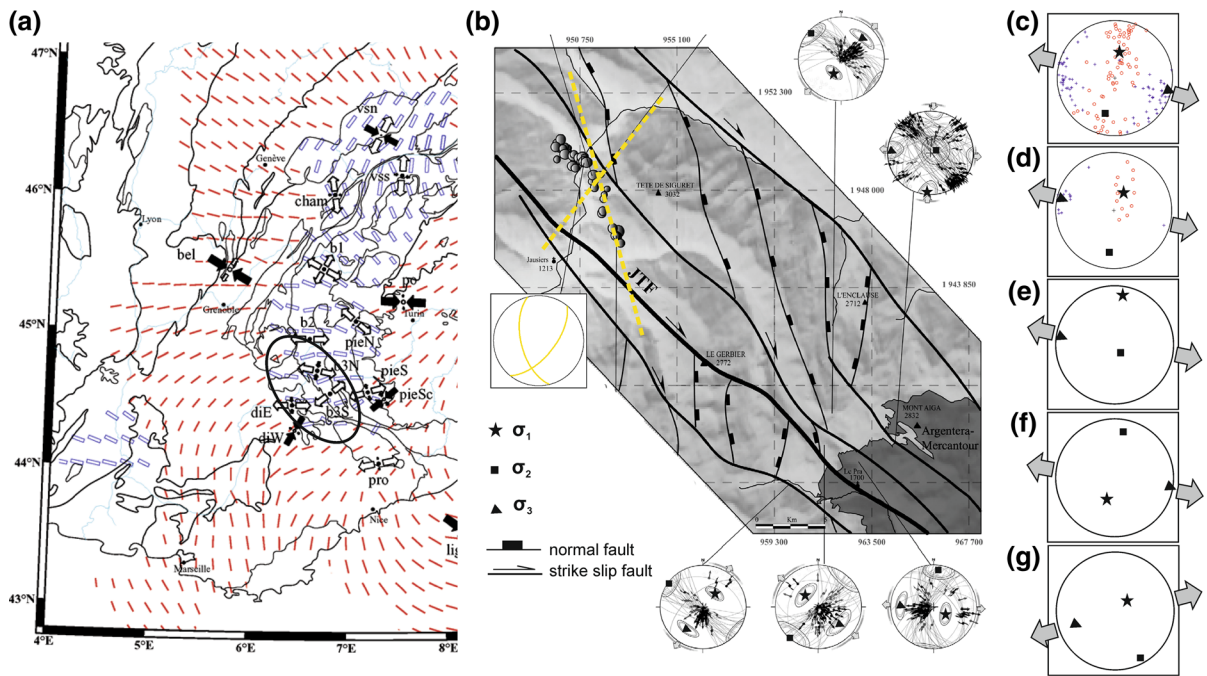
Figure 4
a Map of the Alpine strain/stress state after Delacou (2004). The ellipse indicates the area under study. **b** Geological map with paleostress along the Jausier-Tinée fault (JTF); after Sanchez et al. (2010b). Small circles denote the 74 events of the 2003–2004 swarm under study. The focal mechanism with yellow nodal lines corresponds to principal fault nodal lines. Dashed yellow lines show the orientation of the principal faults found from stress analysis. Positions of the principal axes of tectonic stress retrieved: **c** in the present work for swarm 2003–2004; **d** in the present work for swarm 2012–2015; **e** by Leclère et al. (2012) for swarm 2003–2004; **f** by Delacou et al. (2004) for the Southwestern Brianconnais; **g** by Eva and Solarino (1998) for the western Alps. The grey arrows show directions of extension. Circles/crosses in (**c**, **d**) mark the P/T axes, respectively

significantly deviate from the horizontal plane. However, since their magnitudes are similar, they cannot be retrieved very accurately. By contrast, the accuracy of the orientation of σ_3 is much higher; the σ_3 axis is nearly horizontal and well consistent with previous analyses (see Table 1). The orientation of inclined principal stress axes σ_1 and σ_2 might indicate an inclination of geological structures in the focal zone. The differences in the results obtained by various authors are significant and point to either high uncertainties produced by the stress inversions, or to spatial or temporal variations of relative magnitudes of the σ_1 and σ_2 principal stresses. Since σ_1 and σ_2 have similar values, their axes can easily rotate due to stress uncertainties in the plane perpendicular to the σ_3 direction.

Our results show that the N130°E fault system, suggested by Daniel et al. (2011) as active for the 2003–2004 swarm, is not optimally oriented for

shearing under the present-day stress field. Therefore, this fault is highly unlikely to be activated. A more plausible orientation of the main active fault in the 2003–2004 swarm is obtained by plane fitting to foci of 74 earthquakes analysed by Leclère et al. (2013, their Fig. 6). This plane is striking N155°E being well consistent with the fault plane of the calculated principal focal mechanism for the 2003–2004 seismic swarm (strike 166°, dip 58°, rake − 135°, see Fig. 5a and Table 2). If some events occurred on misoriented fault segments, they should form a minority being probably triggered and strongly influenced by presence of fluids. Moreover, the stress analysis reveals that another system of small faults running in the NE–SW directions has been activated. These faults are also well oriented for shearing under the stress in the region.

A rather low value of static friction of the fault of 0.2–0.3 obtained in the inversion indicates a
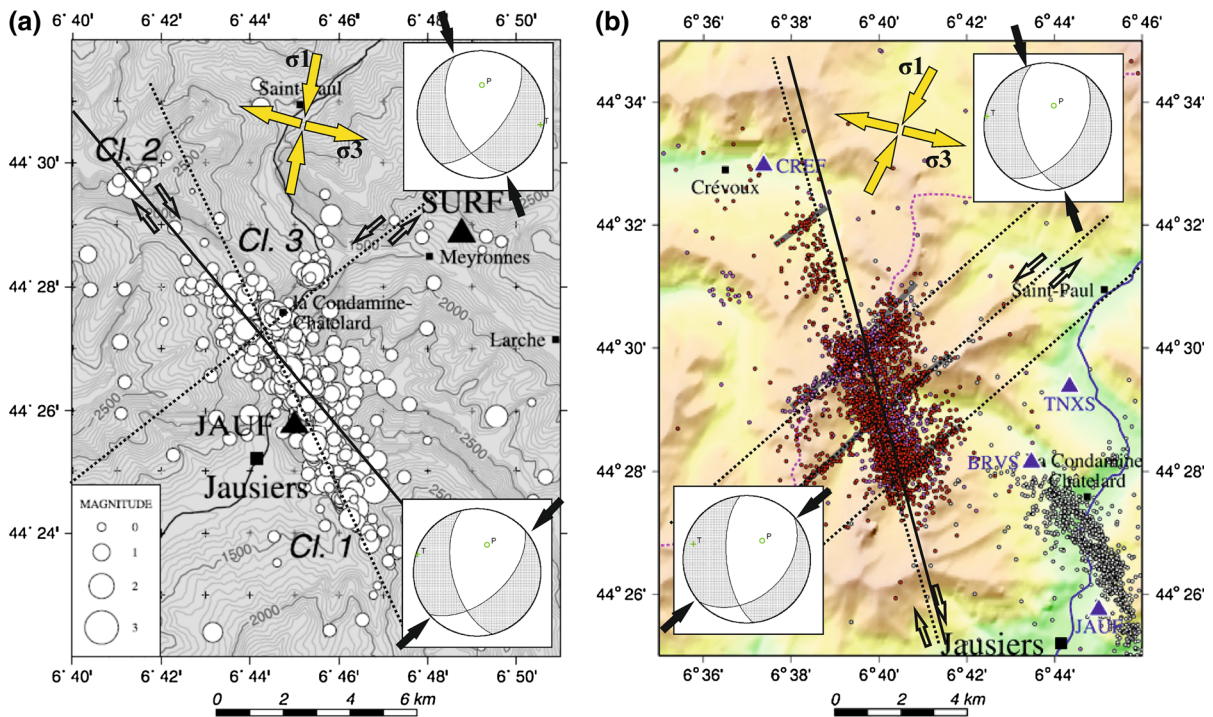
Figure 5
Comparison of seismic swarms 2003–2004 (**a**) and 2012–2015 (**b**). Dots mark the epicentres of the microearthquakes. Solid line denotes the existing fault. The dash lines show the orientation of the principal faults found by the stress analysis. The grey full arrows mark the orientation of tectonic stress retrieved for the both seismic swarms separately. Two focal mechanisms correspond to the principal faults. Principal fault nodal lines are marked by small black arrows. The figures are modified after Jenatton et al. (2007) and Thouvenot et al. (2016)

Table 2

Principal focal mechanisms of the 2003–2004 and 2012–2015 swarms

Swarm	Strike (°)	Dip (°)	Rake (°)
2003–2004	39	61	− 46
	166	58	− 136
2012–2015	37	48	− 51
	174	64	− 129

Note a remarkable similarity of the principal focal mechanisms for both earthquake swarms

reactivation of a preexisting fault in the area under study. This value is lower than usually observed friction on faults but still it is physically acceptable (Sibson 1985, 1994; Scholz 2002). The low value of friction supports the idea that reactivated faults were weak. The apparent weakness of such fault structures seems most likely to arise from locally elevated fluid pressure, rather than from the presence of anomalously low-friction material within the fault zones (Sibson 1996; Vavryčuk and Hrubcová 2017). The Argentera massif is composed of granitoids and gneisses without ultramafic rocks or serpentinite; the presence of very low friction minerals, such as talc or serpentine, is not very likely (Leclère et al. 2012).

For the 2012–2015 swarm, the orientation of the principal stress axes σ_1, σ_2 and σ_3 (azimuth/plunge): 29°/61°, 188°/27° and 283°/9°, respectively, have a similar orientation as for the 2003–2004 swarm (see Table 1). The error of the σ_3 axis is about 10°. The azimuth of the $\sigma_1 - \sigma_2$ plane is of the same accuracy but the error of the plunge of the σ_1 and σ_2 axes within the plane is quite high reaching a value up to 45° at the 95% confidence level (see Fig. 3c). The considerably higher errors of the stress obtained for the 2012–2015 swarm are due to a rather low number of focal mechanisms inverted.

Figure 4c,d indicates that the stress pattern is almost identical for both swarms. In both swarm activities, the σ_3 axis is well constrained being nearly horizontal and the stress ratio is low. As a consequence, the σ_1 and σ_2 principal stresses have similar magnitudes, so the orientations of the σ_1 and σ_2 axes are not well constrained in the plane perpendicular to the σ_3 axis. The orientation of the main fault calculated by fitting hypoDD locations of the 2012–2015 swarm events is characterized by strike of 165°, dip of 80° (Thouvenot et al. 2016). According to these values, the main active fault is favourably oriented for shearing with respect to tectonic stress and close to the principal fault in the region (see Fig. 5b and Table 2). In addition, a system of three small parallel faults running in the NE–SW direction was activated. This system is symmetrically oriented with respect to the maximum compression and coincides with the second principal fault in the region (see Table 2). Having compared the stress pattern and principal focal mechanisms computed for the two studied swarms, we conclude that active faults in the 2003–2004 swarm have very similar orientations as those in the 2012–2015 swarm. A less number of located events in the 2003–2004 swarm and their lower accuracy made more difficult to identify these fault planes by foci fitting (Fig. 5a).

8. Conclusions

The analysis of the 2003–2004 and 2012–2015 earthquake swarms indicates that the tectonic stress regime was similar for both prominent swarms. The σ_3 axis is nearly horizontal with azimuth of $\sim 103°$. This finding is consistent with previous results reported by Leclère et al. (2012). The stress ratio $R \sim 0.2$–0.4 indicates that the principal stresses σ_1 and σ_2 have similar magnitudes. Not only a single fault but also other sub-faults were activated during the seismic activity. The activated faults formed two conjugate fault systems symmetrically inclined from the maximum compression and optimally oriented for shear faulting with respect to tectonic stress. Their orientation differs from that of the major fault system known from geological mapping in the region. The estimated value 0.2–0.3 of friction coefficient at the

faults is quite low and supports an idea of a seismic activity triggered or strongly affected by presence of fluids. The weakness of the fault systems activated during the swarms is also consistent with the predominantly extensional stress regime in the area. Obviously, a more definitive conclusion about the role of fluids can be provided by an accurate analysis of a future seismic activity in this area by determining not only focal mechanisms but also full moment tensors and interpreting their non-double-couple components (see e.g., Vavryčuk and Hrubcová 2017).

REFERENCES

Angelier, J. (1984). Tectonic analysis of fault slip data sets. *Journal of Geophysical Research, 89*(B7), 5835–5848. https://doi.org/10.1029/JB089iB07p05835.

Bott, M. H. P. (1959). The mechanics of oblique slip faulting. *Geological Magazine, 96,* 109–117.

Daniel, G., Prono, E., Renard, F., Thouvenot, F., Hainzl, S., Marsan, D., et al. (2011). Changes in effective stress during the 2003–2004 Ubaye seismic swarm, France. *Journal of Geophysical Research, 116,* B01309. https://doi.org/10.1029/2010JB007551.

Delacou, B., Sue, C., Champagnac, J. D., & Burkhard, M. (2004). Present-day geodynamics in the bend of the western and central Alps as constrained by earthquake analysis. *Geophysical Journal International, 158*(2), 753–774.

Eva, E., & Solarino, S. (1998). Variations of stress directions in the western Alpine arc. *Geophysical Journal International, 135,* 438–448.

Fischer, T., & Horálek, J. (2003). Space-time distribution of earthquake swarms in the principal focal zone of the NW Bohemia/Vogtlandseismoactive region: period 1985–2001. *Journal of Geodynamics, 35,* 125–144.

Fischer, T., Horálek, J., Hrubcová, P., Vavryčuk, V., Brauer, K., & Kampf, H. (2014). Intra-continental earthquake swarms in West-Bohemia and Vogtland: a review. *Tectonophysics, 611,* 1–27. https://doi.org/10.1016/j.tecto.2013.11.001.

Frechet, J., & Pavoni, N. (1979). Etude de la sismicit'e de la zone Brianc¸onnaiseentre Pelvoux etArgentera (AlpesOrientales) a laide dun reseau destations portables. *Eclogae Geologicae Helvetica, 72,* 763–779.

Gephart, J. W., & Forsyth, D. W. (1984). An improved method for determining the regional stress tensor using earthquake focal mechanism data: application to the San Fernando earthquake sequence. *Journal of Geophysical Research, 89*(B11), 9305–9320. https://doi.org/10.1029/JB089iB11p09305.

Got, J. L., Monteiller, V., Guilbert, J., Marsan, D., Cansi, Y., Maillard, C., et al. (2011). Strain localization and fluid migration from earthquake relocation and seismicity analysis in the western Vosges (France). *Geophysical Journal International, 185,* 365–384. https://doi.org/10.1111/j.1365-246X.2011.04944.x.

Guyoton, F., Frechet, J., & Thouvenot, F. (1990). La crise sismique de janvier 1989 en Haute-Ubaye (Alpes-de-Haute-Provence, France): etude fine de la sismicite par le nouveau reseau SISMALP. *Comptes rendus de l'Académie des sciences, Series, 2*(311), 985–991.

Hardebeck, J. L., & Michael, A. J. (2006). Damped regional-scale stress inversions: methodology and examples for southern California and the Coalinga aftershock sequence. *Journal of Geophysical Research, 111,* B11310.

Hensch, M., Riedel, C., Reinhardt, J., & Dahm, T. (2008). Hypocenter migration of fluid-induced earthquake swarms in the Tjörnes Fracture Zone (North Iceland). *Tectonophysics, 447,* 80–94.

Hill, D. P. (1977). A model for earthquake swarms. *Journal of Geophysical Research, 82,* 1347–1352. https://doi.org/10.1029/JB082i008p01347.

Jenatton, L., Guiguet, R., Thouvenot, F., & Daix, N. (2007). The 16,000-event 2003–2004 earthquake swarm in Ubaye (French Alps). *Journal of Geophysical Research, 112,* B11304. https://doi.org/10.1029/2006JB004878.

Labaume, P., Ritz, J. F., & Philip, H. (1989). Failles normales recentes dans les Alpes sud-occidentales: leurs relations avec la tectonique compressive. *Comptes rendus de l'Académie des sciences, Series, 2*(308), 1553–1560.

Larroque, C., Delouis, B., Godel, B., & Nocquet, J. M. (2009). Active deformation at the Southwestern Alps-Ligurian basin junction (France-Italy boundary): evidence for recent change from compression to extension in the Argentera massif. *Tectonophysics, 467,* 22–34.

Leclère, H., Daniel, G., Fabbri, O., Cappa, F., & Thouvenot, F. (2013). Tracking fluid pressure build-up from focal mechanisms during the 2003–2004 Ubaye seismic swarm. *Journal of Geophysical Research, 118,* 4461–4476.

Leclère, H., Fabbri, O., Daniel, G., & Cappa, F. (2012). Reactivation of a strike-slip fault by fluid overpressuring in the southwestern French-Italian Alps. *Geophysical Journal International, 189*(1), 29–37. https://doi.org/10.1111/j.1365-246X.2011.05345.x.

Martinez-Garzón, P., Ben-Zion, Y., Abolfathian, N., Kwiatek, G., & Bohnhoff, M. (2016a). A refined methodology for stress inversions of earthquake focal mechanisms. *Journal of Geophysical Research, Solid Earth, 121,* 8666–8687.

Martinez-Garzón, P., Vavryčuk, V., Kwiatek, G., & Bohnhoff, M. (2016b). Sensitivity of stress inversion of focal mechanisms to pore pressure changes. *Geophysical Research Letters, 43*(16), 8441–8450. https://doi.org/10.1002/2016GL070145.

Maury, J., Cornet, F. H., & Dorbath, L. (2013). A review of methods for determining stress fields from earthquake focal mechanisms: application to the Sierentz 1980 seismic crisis (Upper Rhine graben). *Bulletin de la Societe Geologique de France, 184*(4–5), 319–334.

Michael, A.J. (1984). Determination of stress from slip data: faults and folds. *Journal of Geophysical Research, 89,* 11 517–11 526.

Michael, A. J. (1987). Use of focal mechanisms to determine stress: a control study. *Journal of Geophysical Research, 92*(B1), 357–368.

Nicolas, M., Béthoux, N., & Madeddu, B. (1998). Instrumental seismicity of the Western Alps: a revised catalogue. *Pure and Applied Geophysics, 152,* 707–731.

Reasenberg, P.A., & Oppenheimer, D.H. (1985). FPFIT, FPPLOT and FPPAGE: FORTRAN computer programs for calculating and displaying earthquake fault-plane solutions. U.S. Geological Survey Open File Report, 85–739, 109 pp.

Sanchez, G., Rolland, Y., Corsini, M., Braucher, R., Bourles, D., Arnold, M., et al. (2010a). Relationships between tectonics, slope instability and climate change: cosmic ray exposure dating of active faults, landslides and glacial surfaces in the SW Alps. *Geomorphology, 117,* 1–13.

Sanchez, G., Rolland, Y., Schreiber, D., Giannerini, G., Corsini, M., & Lardeaux, J.-M. (2010b). The active fault system of the SWAlps. *Journal of Geodynamics, 49*(5), 296–302. https://doi.org/10.1016/j.jog.2009.11.009.

Scholz, C. H. (2002). *The mechanics of earthquakes and faulting.* Cambridge: Cambridge University Press.

Shelly, D. R., Hill, D. P., Massin, F., Farrell, J., Smith, R. B., & Taira, T. (2013). A fluid-driven earthquake swarm on the margin of the Yellowstone Caldera. *Journal of Geophysical Research, Solid Earth, 118,* 4872–4886. https://doi.org/10.1002/jgrb.50362.

Sibson, R. H. (1985). A note on fault reactivation. *Journal of Structural Geology, 7,* 75–754.

Sibson, R. H. (1994). An assessment of field evidence for 'Byerlee' friction. *Pure and Applied Geophysics, 42*(3/4), 645–662.

Sibson, R. H. (1996). Structural permeability of fluid-driven fault-fracture meshes. *Journal of Structural Geology, 18*(8), 1031–1042.

Sue, C., Delacou, B., Champagnac, J., Allanic, C., Tricart, P., & Burkhard, M. (2007). Extensional neotectonics around the bend of the Western/CentralAlps: an overview. *International Journal of Earth Sciences, 96,* 1101–1129.

Tesauro, M., Hollenstein, Ch., Egli, R., Geiger, A., & Kahle, H. (2006). Analysis of central western Europe deformation using GPS and seismic data. *Journal of Geodynamics, 42,* 194–209.

Thouvenot, F., Jenatton, L., Scafidi, D., Turino, C., Potin, B., & Ferretti, G. (2016). Encore Ubaye: Earthquake Swarms, Foreshocks, and Aftershocks in the Southern French Alps. *Bulletin of the Seismological Society of America, 106*(5), 2244–2257. https://doi.org/10.1785/0120150249.

Townend, J., Sherburn, S., Arnold, R., Boese, C., & Woods, L. (2012). Three-dimensional variations in present-day tectonic stress along the Australia-Pacific plate boundary in New Zealand. *Earth and Planetary Science Letters, 353–354,* 47–59.

Vavryčuk, V. (2006). Spatially dependent seismic anisotropy in the Tonga subduction zone: a possible contributor to the complexity of deep earthquakes. *Physics of the Earth and Planetary Interiors, 155,* 63–72. https://doi.org/10.1016/j.pepi.2005.10.005.

Vavryčuk, V. (2011). Principal earthquakes: theory and observations from the 2008 West Bohemia swarm. *Earth and Planetary*

Science Letters, 305, 290–296. https://doi.org/10.1016/j.epsl.2011.03.002.

Vavryčuk, V. (2014). Iterative joint inversion for stress and fault orientations from focal mechanisms. *Geophysical Journal International, 199,* 69–77. https://doi.org/10.1093/gji/ggu224.

Vavryčuk, V. (2015). Earthquake mechanisms and stress field. In M. Beer et al. (Ed.), *Encyclopedia of Earthquake Engineering* (pp. 728–746), Springer, Berlin, https://doi.org/10.1007/978-3-642-36197-5_295-1.

Vavryčuk, V., Bouchaala, F., & Fischer, T. (2013). High-resolution fault image from accurate locations and focal mechanisms of the 2008 swarm earthquakes in West Bohemia, Czech Republic. *Tectonophysics, 590,* 189–195. https://doi.org/10.1016/j.tecto.2013.01.025.

Vavryčuk, V., & Hrubcová, P. (2017). Seismological evidence of fault weakening due to erosion by fluids from observations of intraplate earthquake swarms. *Journal of Geophysical Research,* *Solid Earth, 122*(5), 3701–3718. https://doi.org/10.1002/2017JB013958.

Vidale, J. E., Boyle, K. L., & Shearer, P. M. (2006). Crustal earthquake bursts in California and Japan: their patterns and relation to volcanoes. *Journal of Geophysical Research, 33,* L20313. https://doi.org/10.1029/2006GL027723.

Wallace, R. E. (1951). Geometry of shearing stress and relation to faulting. *Journal of Geology, 59,* 118–130. https://doi.org/10.1086/625831.

Yoshida, K., Hasegawa, A., & Yoshida, T. (2016). Temporal variation of frictional strength in an earthquake swarm in NE Japan caused by fluid migration. *Journal of Geophysical Research, Solid Earth, 121,* 5953–5965. https://doi.org/10.1002/2016JB013022.

Zoback, M. L. (1992). First- and second-order patterns of stress in the lithosphere: the world stress map project. *Journal of Geophysical Research, 97*(B8), 11703–11728. https://doi.org/10.1029/92JB00132.